A SEARCH FOR THE FIRST EXCITED STATE OF ^{57}CU

by

Stephen E. Hale Jr.

University Undergraduate Fellow, 1992-1993

Texas A&M University

Department of Physics

APPROVED

Fellows Advisor Robert C. Tribble

Honors Director

Table of Contents

Chapter		Page
I.	INTRODUCTION	1
II.	BACKGROUND OF NUCLEAR PHYSICS	3
	A. Shell Model of the Nucleus	3
	B. Nuclear Decay	7
	C. Importance of ^{57}Cu	9
III.	EXPERIMENTAL PROCESS	13
	A. Transport Through MARS	13
	B. Detector System Set-Up	16
	C. Electronics Set-Up	18
IV.	DATA ANALYSIS	20
V.	RESULTS AND CONCLUSIONS	22
	A. Performance of the System	22
	B. Identification of ^{57}Cu	25
	C. Conclusions and Future Plans	27
	APPENDIX A: Results of April Run	28

List of Figures

Figure		Page
1.	Energy levels for neutrons and protons in a nuclear potential well (schematic).	3
2.	Comparison of levels in an infinite potential well with spin-orbit coupling level sequence.	5
3.	The parity operator ($x \rightarrow -x$, $y \rightarrow -y$, $z \rightarrow -z$).	5
4.	Diagram of rp-process demonstrating the crucial role played by ^{56}Ni.	12
5.	Schematic outline of the Momentum Achromat Recoil Spectrometer (MARS).	14
6.	Electronics set-up schematic for MARS ^{57}Cu run.	18
7.	POS vs. DE for run with 2 inch slits.	23
8.	POS vs. DE for run with 1 inch slits.	24
9.	POS vs. E for run with 2 inch slits.	25
10.	POS vs. E for run with 1 inch slits.	26
A1.	POS vs. E for sum of four runs.	29

List of Tables

Table		Page
1.	"Magic" Numbers of Protons and Neutrons	6
2.	Electromagnetic Multipole Transitions	8

I. Introduction

The nucleus ^{57}Cu plays an important role in several areas of nuclear physics, including Coulomb displacement calculations and nuclear astrophysics. Recent work concerning ^{57}Cu has revealed details about this nucleus. The mass excess has been determined to within 15 keV.[1] An excited state has been found at 1.04±0.04 MeV, although its spin and parity has not been determined.[2] Rough measurements have been made of the half-life (^{57}Cu decays to ^{57}Ni by β-decay) and of the branching ratios to the ^{57}Ni ground and 1.113 MeV $2p_{1/2}$ states.[3]

The objective of this project is to determine more about the exited states of ^{57}Cu using the Momentum Achromat Recoil Spectrometer (MARS) located at the Texas A&M Cyclotron Institute. Using γ-ray detectors at the target chamber with a coincidence circuit to identify ^{57}Cu at the focal plane, we will attempt to locate the $2p_{1/2}$ state which plays a crucial role in determining the nuclear synthesis of proton-rich elements more massive than ^{56}Ni.

The results presented in this paper are preliminary data recorded during the experiment conducted from December 16 to December 19, 1992. During this experimental run, major problems developed in the velocity filter, a primary component of MARS used to separate the ^{57}Cu from background products. The data that was recorded has been used to analyze the

characteristics of the system. A run is scheduled for April 9 to April 13, 1993, to continue the search for the energy levels of ^{57}Cu.

II. Background of Nuclear Physics

There are several models of nuclear structure in use today. Different models have various characteristics which make them particularly useful for a variety of situations.

Shell Model of the Nucleus

The shell model of nuclei describes the system of neutrons and protons in a manner similar to the atomic electron orbital shells. With two distinct particles in the nucleus, however, there are two sets of shells which must be kept track of separately. Figure 1 shows a schematic of the energy for both protons and neutrons in a nuclear potential well.

Figure 1: Energy levels for neutrons and protons in a nuclear potential well (schematic).

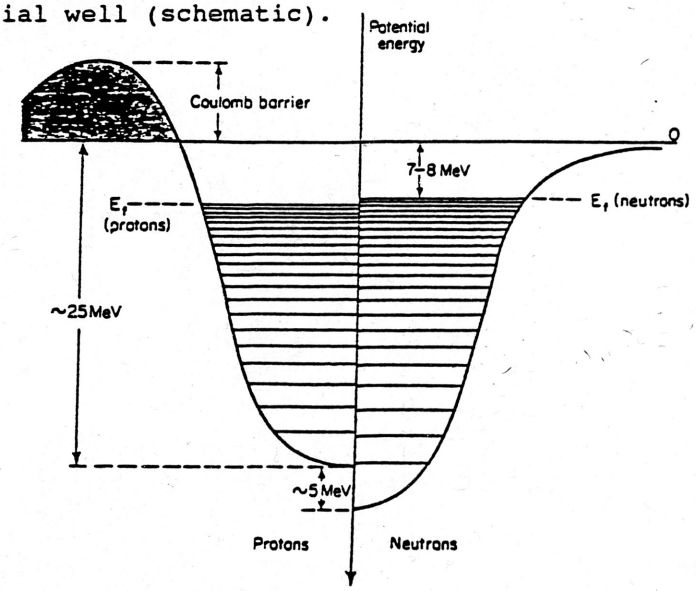

Source: B. G. Harvey. *Introduction to Nuclear Physics and Chemistry*. p. 116.

The energy levels, or states, of the nucleus are labeled in a specific fashion. A typical state would be $2p_{1/2^-}$. The first number refers to the orbital that the nucleon is in. It is denoted as n and is called the principle quantum number. The letter, p in this case, denotes the orbital angular momentum, ℓ, that the nucleon has. These labels go in the order of: s, p, d, f, g, h, etc., and they correspond to ℓ values of 0, 1, 2, 3, 4, 5, 6, etc., measured in units of $\hbar$, Planck's constant. The fractional subscript represents the total angular momentum in each orbital and is a coupling of the orbital angular momentum, ℓ, and the spin angular momentum, $\frac{1}{2}$, to $\ell \pm \frac{1}{2}$. In the shell model, the two angular momenta for each ℓ are split by a spin-orbit force whose origin from the nucleon-nucleon force is not understood.[4] The $\ell - \frac{1}{2}$ member of each pair corresponds to a more energetic orbital than the $\ell + \frac{1}{2}$ member. A typical ordering of states is given in Figure 2.

Finally, the ± sign following the spin-orbit splitting term denotes the parity of the state. An odd parity is denoted by - while an even parity is denoted by +. The value of the parity is given by $(-1)^{\ell}$. A way to visualize parity is that an even parity system is equal to its inversion ($x \rightarrow -x$, $y \rightarrow -y$, $z \rightarrow -z$)while an odd parity system is equal to the negative of its inversion. Figure 3 shows the effect of the parity operator.

Figure 2: Comparison of levels in an infinite potential well with spin-orbit coupling level sequence.

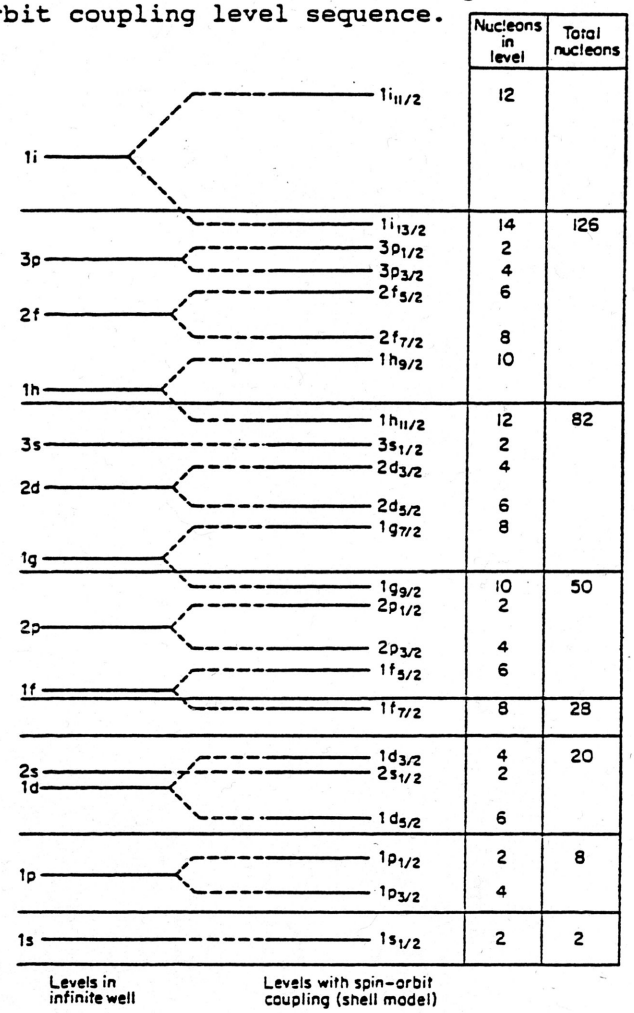

Source: B. G. Harvey. *Introduction to Nuclear Physics and Chemistry*. p. 124.

Figure 3: The parity operator (x → -x, y → -y, z → -z).

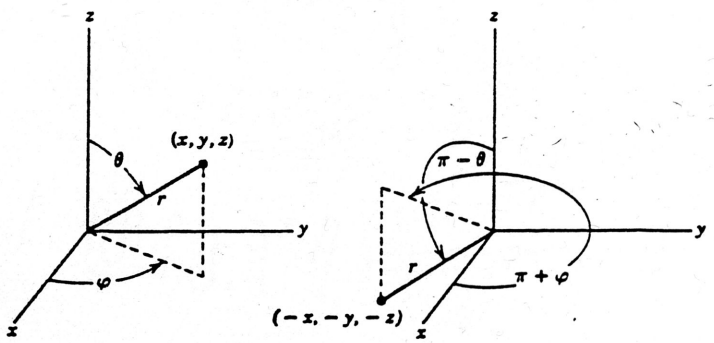

Source: R. Eisberg and R. Resnick. *Quantum Physics of Atoms, Molecules, Solids, Nuclei, and Particles*. p. 294.

Also analogous to e^- orbital shells, there are specific numbers of protons and neutrons which have stable energetic configurations. With the two species of nuclear particles, there are nuclei which have special numbers of neutrons or protons or both. Such nuclei are referred to as "magic nuclei", or "doubly magic" in the case of simultaneous special numbers of protons and neutrons. Table 1 shows the "magic" numbers for nucleons.

Table 1: "Magic" Numbers of Protons and Neutrons

Protons	Neutrons
2	2
8	8
20	20
28	28
50	50
82	82
126	126

The ^{56}Ni nucleus is one of these "doubly magic" configurations. Its 28 protons and 28 neutrons form a very stable state. Nuclei with one more particle, either a proton or a neutron, above a stable nucleus are referred to as single particle nuclei. ^{57}Cu and ^{57}Ni, with one additional proton and one additional neutron respectively, are examples of these nuclei. They are called mirror nuclei because, neglecting the Coulomb interactions of the protons, the extra neutron and proton behave in a similar manner. Because of this similarity, the energy levels of the strong nuclear force are nearly equivalent. The shift in energy caused by the electromagnetic force from the proton's charge can be treated as a small perturbation to the energy levels.

Nuclear Decay

A nucleus can exist in an excited state by having one of its protons or neutrons, referred to generally as nucleons, raised to a shell out of the ground state configuration. In one method of decay, γ-decay, the nucleon can drop to a lower energy level emitting a photon. The energy of this photon is the difference of the initial and final energy levels of the nucleon. The energies of the photons emitted range upward from about 100 keV, which is the γ-ray energy range of the electromagnetic spectrum.

The γ-decay transition rate can be measured directly or indirectly from the lifetime, T, of the excited state. If $T>10^{-10}$ seconds, then it can be determined by electronically timing the average delay between the excitation of a state and its decay.[5] If T is shorter than 10^{-10} seconds, the energy spread of the emitted γ-rays can be measured, which then leads to a value for T from the energy-time uncertainty principle

$$\Delta T * \Delta E \geq \hbar/2.$$

γ-decay occurs through various types of electromagnetic radiation, such as electric and magnetic dipole, quadrupole, and octupole radiation. These generally have decreasing probabilities in the order given in Table 2,

Table 2: Electromagnetic Multipole Transitions

Transition	L
Electric dipole	1
Magnetic dipole	1
Electric quadrupole	2
Magnetic quadrupole	2
Electric octupole	3
Magnetic octupole	3

where the integer L labels the multipolarity of the transition, which determines the γ-decay selection rules, or allowed transitions. L is also the measure of angular momentum carried away by the γ-ray in units of $\hbar$. The requirement that angular momentum be conserved in γ-decay relates L to the nuclear spins, while the symmetry requirement of the transition operator relates L to the nuclear parities. Together these relations lead to the following selection rules:[6]

For electric transitions
$|i_i - i_f| \leq L \leq i_i + i_f$
(but not i_i=0 to i_f=0).
The nuclear parity must change if L is odd and it must not change if L is even.

For magnetic transitions
$|i_i - i_f| \leq L \leq i_i + i_f$
(but not i_i=0 to i_f=0).
The nuclear parity must change if L is even and it must not change if L is odd.

This notation has i_i as the nuclear spin of the initial state and i_f as the nuclear spin of the final state. For single particle nuclei, the dominating transition, i.e. that with the largest transition rate, will have $L = |i_i - i_f|$. If this is odd, the transition will be electric when the initial and final states have opposite parity and magnetic when the

initial and final states have the same parity. If L is even, the opposite is true.

The radiation from the nuclear decay can be identified from transition rate measurements. Thus, information about the spins and parities of the nuclear states can be determined.

Importance of ^{57}Cu

The creation of elements heavier than lithium takes place in stellar cores by nucleosynthesis. At the high temperatures and densities at the center of stars, light atoms fuse together producing heavier elements and energy that supports the star against the gravitational attraction that pulls it towards the center. In very massive stars, the pressure at the core will fuse the elements in a series of chain reactions starting with hydrogen and then using the nuclear "ash" in subsequent reactions. In this process, the nuclear burning follows the path from hydrogen to helium, carbon, neon, oxygen, silicon, and ending with a mixture of iron and nickel. Shells form in an onion-like structure in which the fusion of lighter elements still takes place in the outer-most shells. Nuclei in the iron and nickel region have the highest binding energy so fusing these elements requires energy instead of producing it. Thus the process of nucleosynthesis comes to a halt and an inert core forms. Elements more massive than Fe or Ni must be produced by some other method.[7]

After a star's core of Fe and Ni has grown to the Chandrasekhar mass, the gravitational attraction pulling the inert core towards the center overcomes the pressure generated by the repulsion the Fe and Ni atoms experience. During the collapse that follows, the outer shells of still fusing material fall in. After approximately 1 second, the density of the core becomes greater than normal nuclear density, $\rho_o=10^{14}$ gm/cm^3 [8], and thus the material becomes nearly incompressible. The infalling material strikes the now unyielding core and rebounds, as the core itself also expands slightly from its overcompressed state. This is purported to be the mechanism which forms a Type II supernova.

In the explosion that follows, the nuclear material in the shell of the star is compressed to high density and temperature and a large flux of neutrons and protons is produced. It is in this environment that nucleosynthesis of atoms past Fe and Ni occurs. The classic r, for rapid, process takes place in which nuclei absorb up to 5 or 6 neutrons before beta-decaying back to stable states.[9] The rp, or rapid proton, capture process is the proton analog of the r process. However, the proton series generally stops after absorbing one proton until a decay can occur.

The stability and long half-life of ^{56}Ni make it a major branch point in the rp process.[10] Only after a $^{56}Ni(p,\gamma)^{57}Cu$ proton capture reaction occurs can heavier nuclei be produced. The rate of this reaction is very sensitive to the ^{57}Cu analog

of the 1.113 MeV $2p_{1/2}$ state in ^{57}Ni. At high temperatures, the reaction rate is dependent on the excitation energy and γ-width of the ^{57}Cu analog of the 2.443 MeV $1f_{5/2}$ state in ^{56}Ni.[11] The rp process, along with the crucial step involving ^{56}Ni, is shown in Figure 4.

Another area in which knowledge about the energy levels of ^{57}Cu is useful is the comparison of calculated and experimental Coulomb displacement energies. The result of the accumulated positive charge from the protons is to change the energy levels for the proton system.

^{57}Cu is special in that it can be considered to be a good single particle nucleus. This simple structure facilitates precise calculations of Coulomb displacement energies which can be compared to experimental results to judge the validity of the underlying theory.

Figure 4: Diagram of rp-process demonstrating the crucial role played by ^{56}Ni.

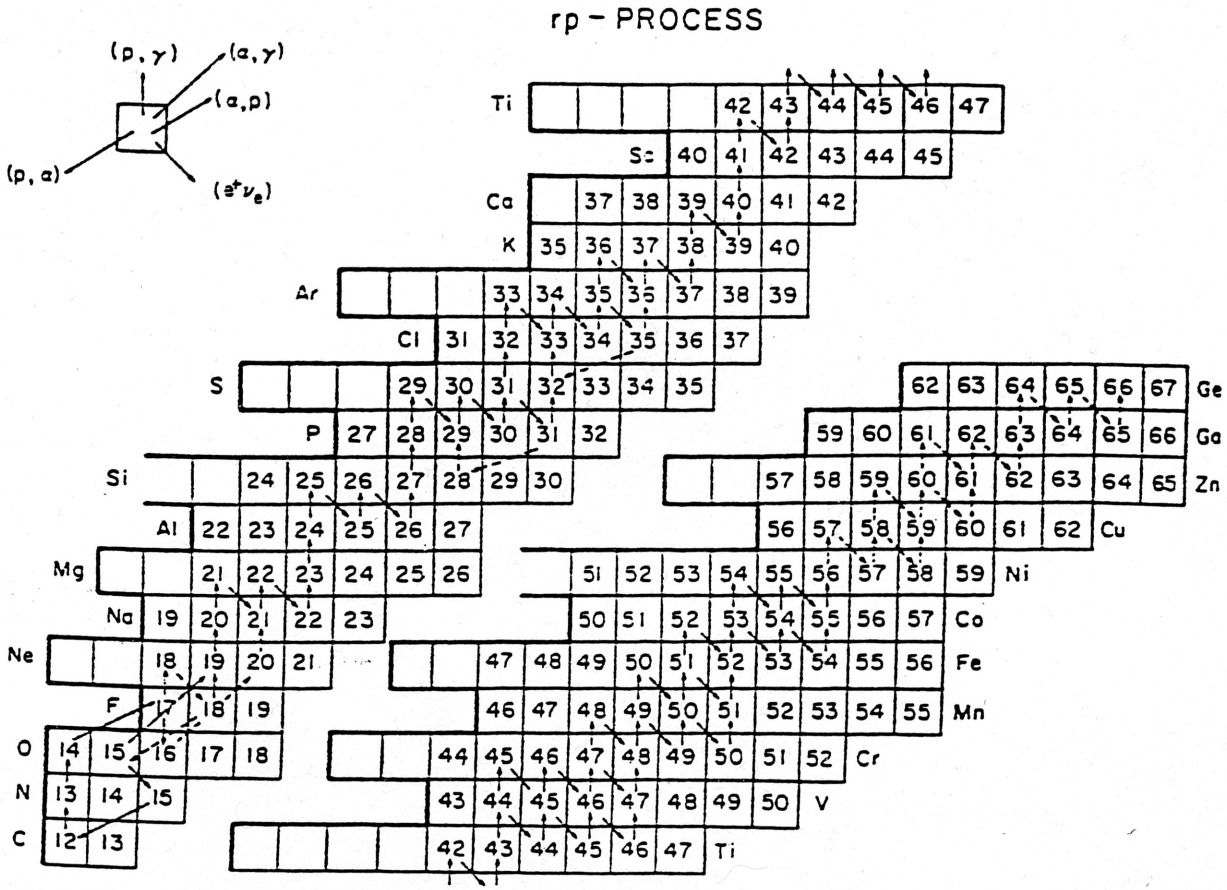

Source: R. K. Wallace and S. E. Woosley, Astrophys. J. Suppl. 45, 392 (1981).

III. Experimental Process

The ^{57}Cu is produced using a ^{58}Ni beam accelerated by the K500 Cyclotron. The nickel beam has an energy of 29 MeV per nucleon, or about 1682 MeV per nucleus. The nickel ions are transported from the K500 to the target chamber of MARS where they are incident on a target of polyethylene, chains of CH_2, with a thickness of 4 mils (1 mil = 0.001 inch) or about 0.01 cm. The ^{58}Ni forms ^{57}Cu via a (p,2n) reaction, $^{58}Ni(p,2n)^{57}Cu$. The reaction requires 21.458 MeV, giving a threshold energy for the reaction to occur.

Transport Through MARS

The products of the various reactions are transported through MARS, the layout of which is shown in Figure 5. After the target chamber, the nuclei travel through quadrupoles 1 and 2 and into dipole 1. The magnetic field of dipole 1 spreads the products horizontally producing a p/q (momentum divided by charge) dispersion because of the force exerted by magnetic fields. Due to the optics of MARS, this dispersion is a maximum at the entrance to quadrupole magnet Q3. Directly after the dipole, the products enter a chamber containing Faraday cups. These are mounted on screw threads which allow their movement across the beam direction. By moving across the beam, the cups will intersect different

Figure 5: Schematic outline of the Momentum Achromat Recoil Spectrometer (MARS).

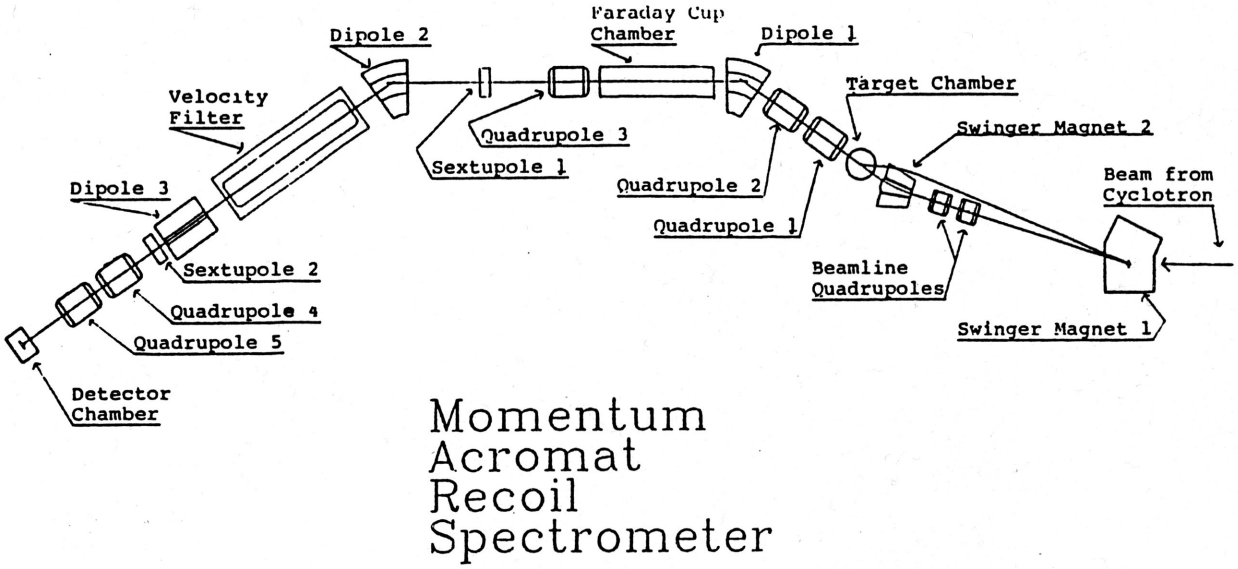

Source: Adapted from D. H. Youngblood, et. al. *Momentum Achromat Recoil Spectrometer: A Proposal to Supplement Grant DE-FG-05-86ER40256*. p. 47.

sections of the horizontally dispersed products, which provides a measure of the beam intensity. The products that we do not want to have present, including the incident ^{58}Ni beam, are separated from the beam by adjusting the cups to change the momentum acceptance of the system.

After passing through Q3, sextupole S1, and dipole D2, the beam enters the velocity filter. Inside the velocity filter there are a set of plates for producing an electric field and a set of coils for producing a magnetic field. The plates carry a positive charge on stainless steel plates on top and a negative charge on anodized aluminum plates on the bottom, separated by a 10 cm gap. With the electric field pointing from positive to negative, the positive ^{57}Cu ions are

displaced downwards according to the expression

$$\bar{F} = q * \bar{E}$$

The coils are arranged to provide a magnetic field perpendicular to the electric field and in such a direction that the force experienced by the ions is in the opposite direction to the electric force. The equation describing this force is

$$\bar{F} = q * (\bar{v} \times \bar{B}).$$

Since the particles are pushed down with a force proportional to their charge, but are also pushed up with a force proportional to their charge times their velocity, the net force is dependent on the velocity of particles and the field settings. By balancing the electric and magnetic fields, a certain velocity can be allowed to pass. The velocity filter thus disperses the beam vertically depending on the magnitude of the particle's velocities.

Directly after the velocity filter, the beam enters the third dipole which, being oriented vertically, bends the beam up. Quadrupoles 4 and 5 focus the beam in the vertical and horizontal planes so that the products are separated at the focal plane detectors. These last three elements are adjusted to reverse the momentum dispersion caused by the velocity filter, to provide a m/q separation.

Detector System Set-up

Because the time-of-flight through MARS for the ^{57}Cu is long compared to the half-life of the excited state, the detectors to observe the γ-rays of the nuclear decay are located at the target chamber. These are intrinsic solid-state germanium detectors. A bias voltage is applied to the detector element in order to draw all of the free electrons out of the material. Then when a high-energy photon passes through the detector, it interacts with the electrons still present in the chemical bonds. The electrons that are knocked loose by the photon are drawn to the sides of the material because of the bias voltage. The current thus generated is detected and, through the electronic circuitry of the detector's built-in preamplifier, is converted into a voltage. This voltage is proportional to the energy of the photon that was originally incident on the detector if the entire photon energy is deposited in the detector. The voltage produced is sent through the electronics system.

At the end of the MARS line there are two other detectors, a single-wire proportional counter and a solid-state silicon detector. The wire proportional counter is a box with a single resistive wire passing vertically through the middle. The box has a negative charge while the wire is at ground potential. The voltage difference between the wire and the box is 780 volts. The box is filled with gas consisting of 10% methane and 90% argon. When particles from the beam

pass through the gas they collide with the gaseous atoms and create ions and electrons. The electrons flow towards the center wire while the ions move towards the shell. The electrons strike the wire and create a current which moves both up and down the wire. The current is split because, by being located in a certain position along the wire, there are different resistance paths that can be traveled. By detecting the difference in the charge on the up versus the down readout, the position of the ions, and thus the position of the beam particle creating the ions, can be determined. Knowing the position of the beam particle allows us to determine what the particle's m/q ratio is because of the dispersion caused by the velocity filter and the bend of the particles by D3. The total number of electrons which strike the wire gives a measure of the differential energy lost by the particles in the detector. Thus the single-wire proportional counter tells us the position and differential energy loss of the beam particle which serve as identifiers of the particle type.

The intrinsic solid-state silicon detector absorbs the particles completely. A bias voltage of 150 volts is applied to draw the electrons which are knocked loose by the incident particles to the sides of the detector. Since the particles will stop inside of the detector, the signal from the silicon detector will indicate the total energy of the particle.

Electronics Set-Up

Figure 6 shows a schematic of the electronics set-up that was used for the December run.

Figure 6: Electronics set-up schematic for MARS ^{57}Cu run.

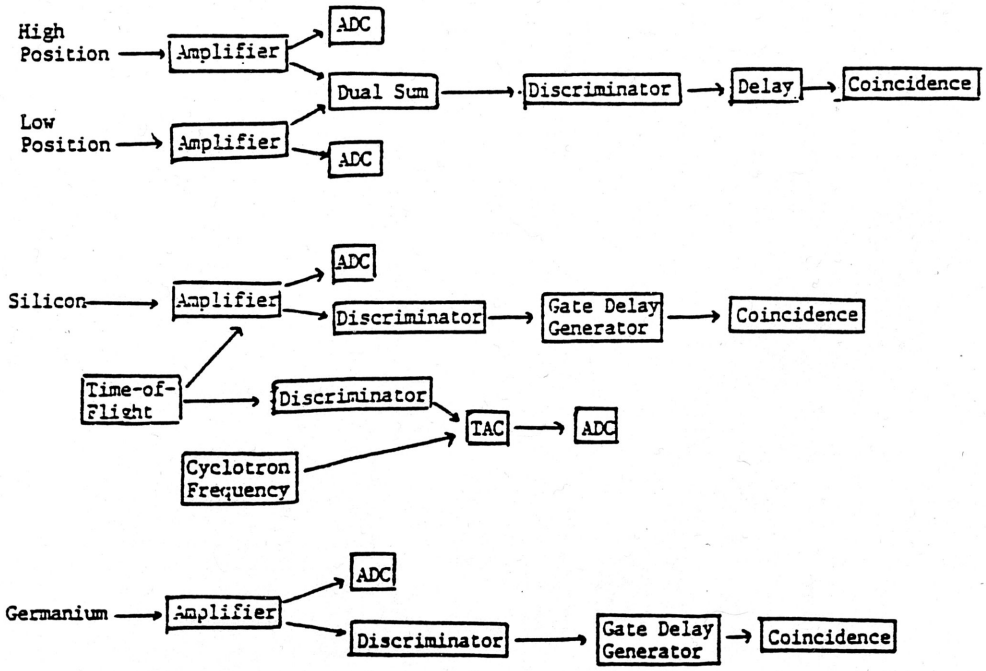

The preamplifier signals from the all of the detectors are input into amplifiers in the computer room. The signal from the amplifiers is immediately put into an Analog to Digital Converter (ADC) which transforms the voltage pulse into a digital signal suitable for the computer. The subsequent paths of the signals are designed to provide a means to select specific events.

Two signals come from the wire detector, a high and a low position reading. These are added together in the dual sum unit and then sent to a discriminator. The discriminator

provides a threshold value check in order to screen out small signals. Those pulses which are above the limiting value are sent through a delay generator, which is adjusted to get the proper timing for the signals, and then into a coincidence unit. The coincidence unit uses the signals from the detectors to select only values which occur simultaneously, taking into account the transit time of the signals through the electronics.

In the sub-system for the silicon detector, a timing signal from a fast timing discriminator and the signal generated by the Cyclotron radio-frequency system are compared to provide another test for particle identification. A coincidence between the silicon detector and the germanium detector is formed through a discriminator-delay generator sequence which leads into a coincidence unit. A fast coincidence between these two detectors is produced by sending the fast timing discriminator signal into a Time to Amplitude Converter (TAC). This output is then put into an ADC.

The digital signals produced in the ADC units are sent to a Micro-programmable Branch Driver (MBD) unit which accepts data characterized as specific types of events. When the buffers of the MBD are full, or when the system is prompted, the MBD dumps the data into the computer analysis and storage system. From there it is analyzed and studied using the Q data acquisition and replay system to provide the results of the experiment.

IV. Data Analysis

The three quantities measured by the detectors at the focal plane, position (POS), differential energy loss (DE), and total energy (E), along with a fourth, the time of flight of the particles as measured versus the cyclotron frequency, provide a means to identify the particle that is observed. A FORTRAN program called DEDX predicts the amounts of energy lost by the beams of particles, depending on the total energy of the beam, as they pass through the detector component parts. These predictions are used to help identify the particles by the output of differential energy loss. By accumulating data on the ^{58}Ni beam, which was done in the mid-December run, the focal plane detectors were calibrated for DE, E, and POS.

The spectra of data that is produced is displayed as histograms such as POS, E, and DE. Combining these into 2-dimensional graphs, for example POS vs. E and POS vs. DE, provides a graphical output which demonstrates the clustering of similar types of particles. The positions of the groups of particles are compared to the calculated values based on the DEDX program and the calibration from ^{58}Ni. By setting gates, or regions of acceptable data, on the cluster identified as ^{57}Cu, the data can be run through the Q system again to select only the data in the germanium energy spectrum that is

coincident with the ^{57}Cu cluster. The coincidence requirement leads to a reduction in the background from random signals. By setting gates in areas of the spectra where data is not expected, a value can be obtained for the background from misidentified particles. These arise because of the spread in energies and energy losses that occur for all of the particles, and can lead to non-^{57}Cu particles being included in a gate set for ^{57}Cu data. The background can then be compared to the experimental results. If a γ-line is observed in our data, it is necessary to check for the presence of the line in the background, for if the line is from the background, it is not the value that we are looking for.

V. Results and Conclusions

The data that is presented was collected in the December 1992 run. During this run, the velocity filter's electric field plates were experiencing difficulties holding a stable voltage. The highest expected voltage for the system is a total of 500 kV, with +250 kV on the top plate and -250 kV on the bottom plate. The plates reached a maximum value of 220 kV, with about a ± 110 kV split between the plates, before serious internal sparking started occurring. The lower voltage reduced the resolution of the experiment because, with an appropriately adjusted magnetic field, there was not as much spread in particle distribution as was desired.

During the run, four data collection recordings were conducted. Three of these had the slits directly before quadrupole 3 changed for each recording in order to see what width would optimize the observation of ^{57}Cu. The data that was recorded from these runs has been analyzed in an attempt to determine the performance of the system and to identify the particle groups.

Performance of the System

The plots of POS v. DE (POSDE) result from the two signals derived from the wire-counter detector. On the POSDE graphs, isotopes should occur along cluster lines slanting

down from left to right, in order of decreasing m/q. This structure can be seen in Figures 7 and 8, which display the POSDE data for the runs with 2 inch and 1 inch slits respectively (the maximum slit width is 8 inches and the third analyzed run had the slit set at 4 inches). However, in both

Figure 7: POS vs. DE for run with 2 inch slits.

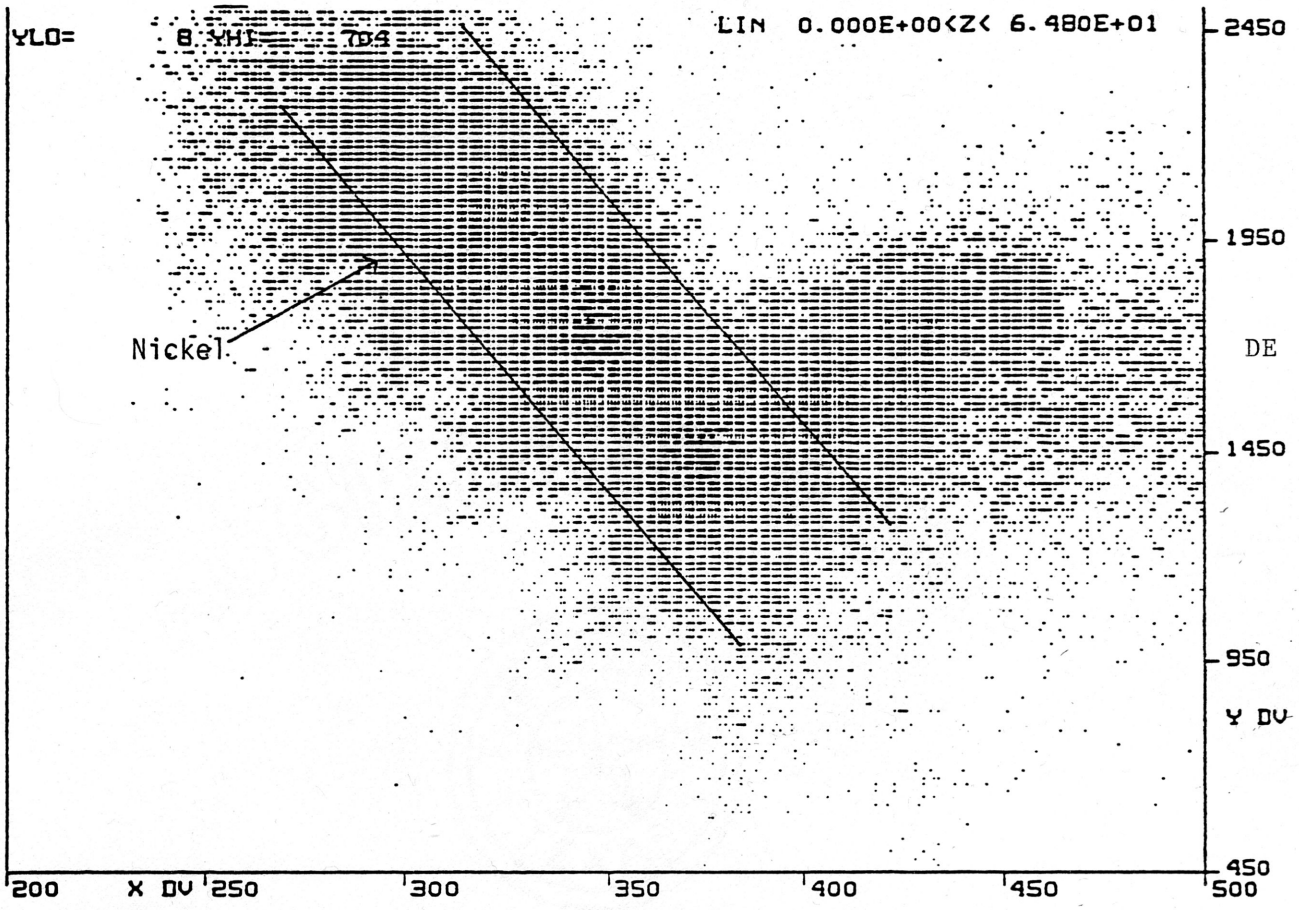

graphs, there is a definite upswing in the data. There should be parallel slanted lines of clusters with each line relating to a different atom. The distinctive line present in both of these graphs has been identified as Ni.

Figure 8: POS vs. DE for run with 1 inch slits.

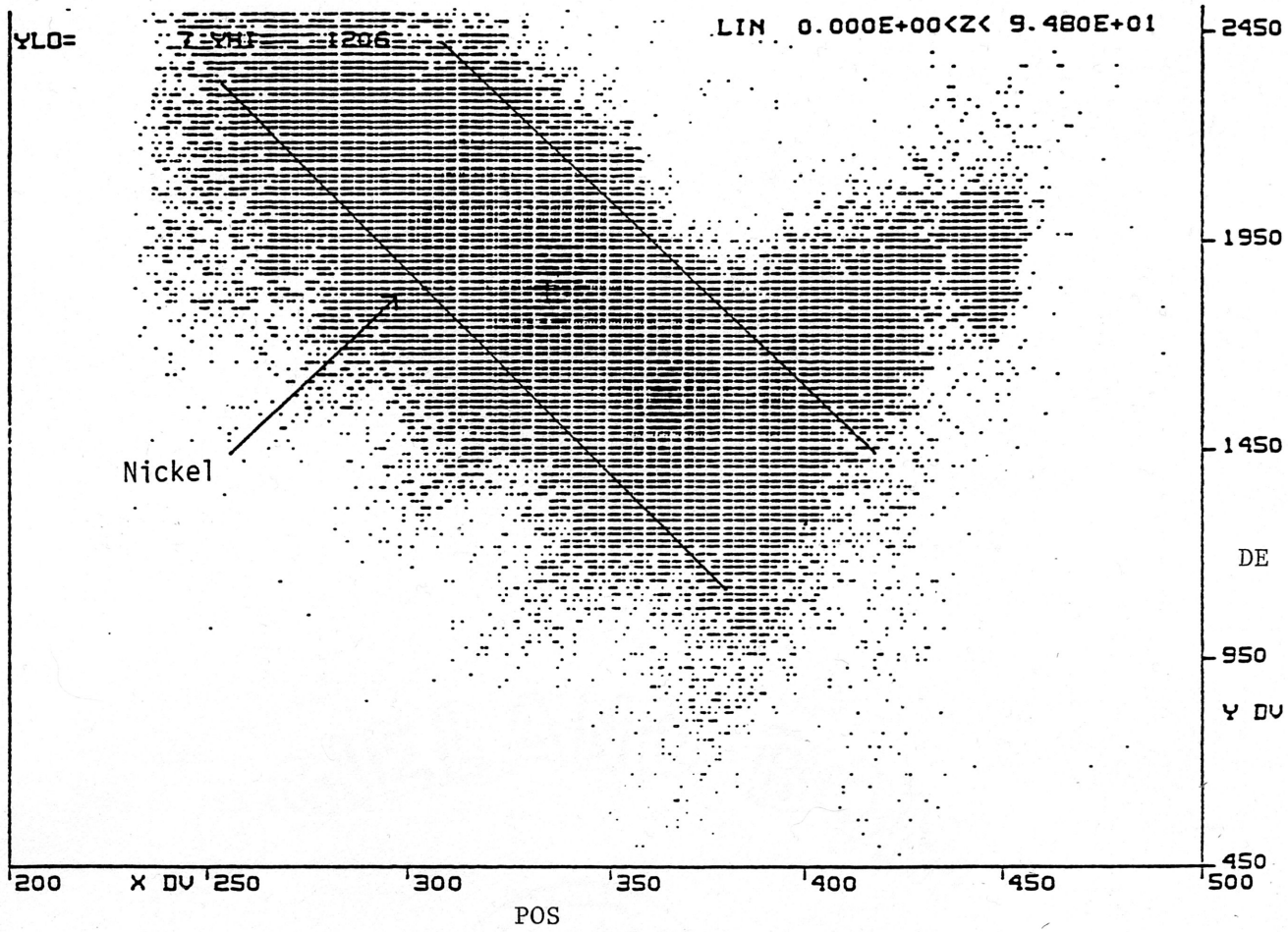

The data present in the upswing is some isotopes of Cu. The missing higher clusters for the Cu line identifies a problem arising in the wire-counter. The large flux of highly charged particles is saturating the counter. Thus the signals out of the counter are not stable and do not give a good measure of the differential energy loss of the particle.

Identification of ^{57}Cu

The POS v. E (POSE) graphs in Figures 9 and 10 (again for slit width 2 inches and 1 inch, respectively) also show clusters of particles. With different slit widths, the two graphs show the particles with different energies that are getting through to the detectors. The DEDX program predicts the amount of energy lost by various background particles in the silicon detector. With the scale set by the ^{58}Ni data, it is possible to establish the identity of the ^{57}Cu group, as is indicated on the plots. The effect of the slit widths is

Figure 9: POS vs. E for run with 2 inch slits.

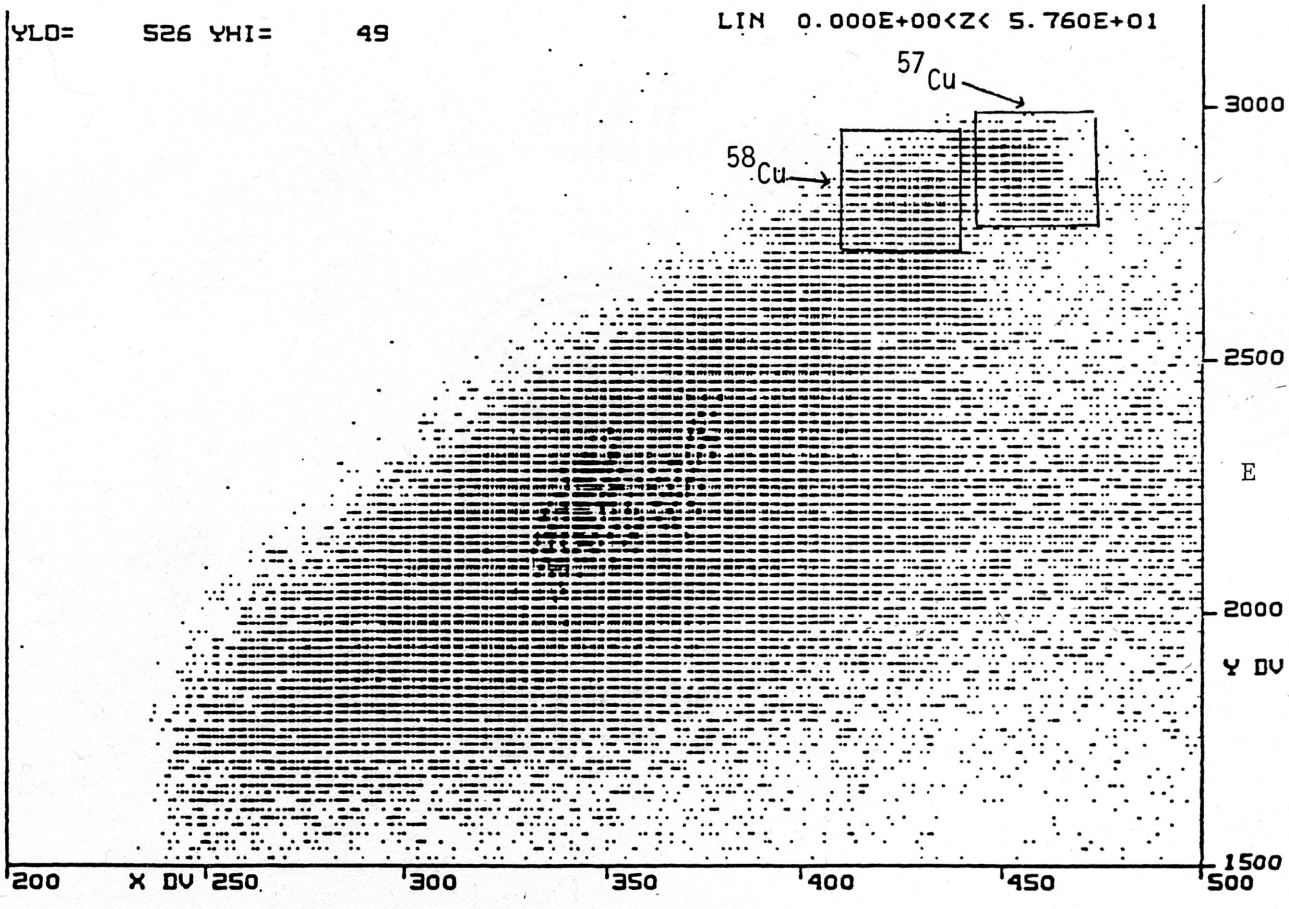

POS

demonstrated by the appearance of the ^{58}Cu in the 2 inch data but not in the 1 inch data. The group of ^{57}Cu can now be gated in order to run the data again selecting only the relevant germanium γ-rays.

Figure 10: POS vs. E for run with 1 inch slits.

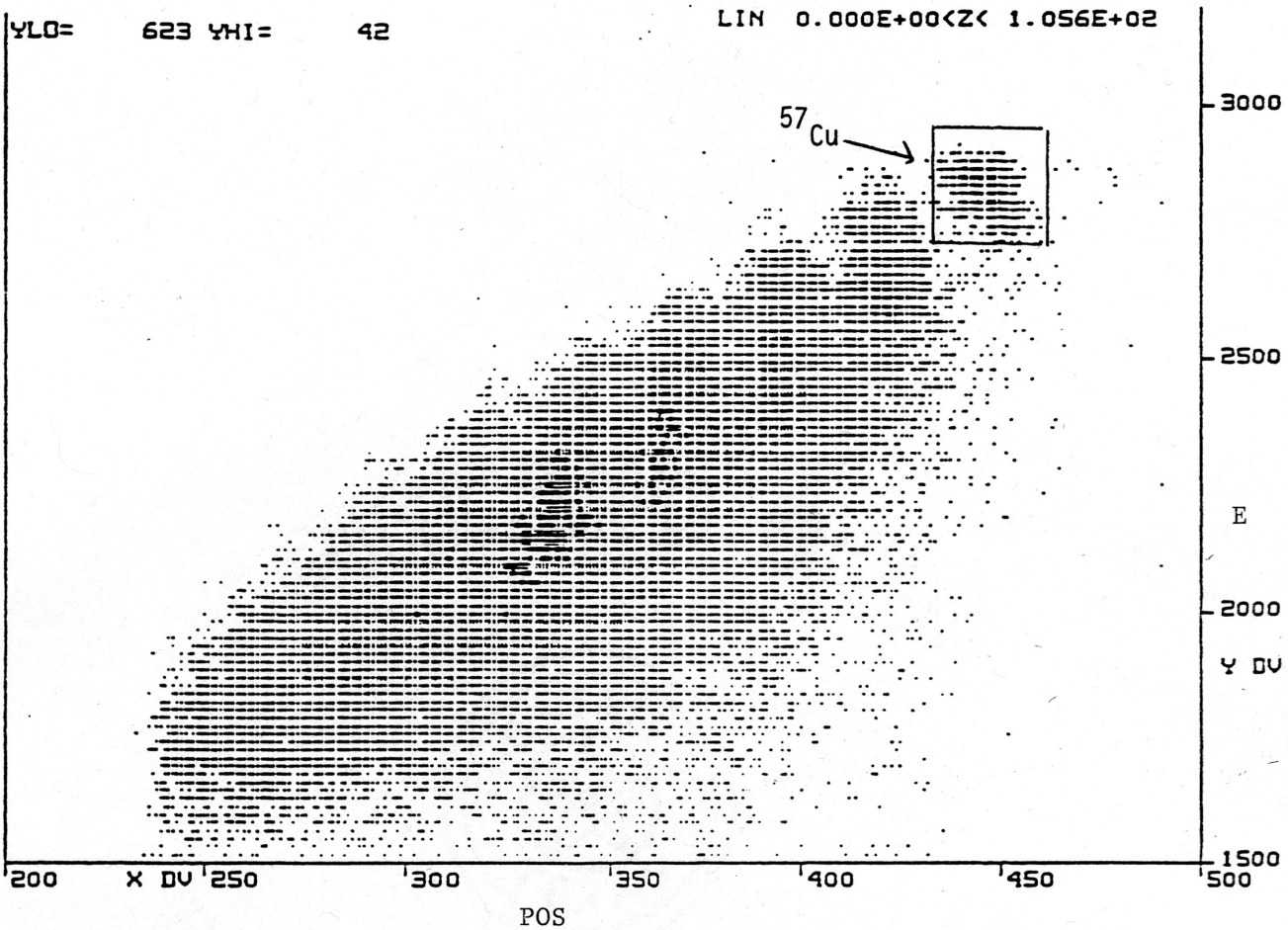

Conclusions and Future Plans

Since the December run, several attempts have been made to alleviate the problem of the sparking of the velocity filter. In preparing for the run from April 9 to April 13 we have been able to raise the potential difference to 260 kV. Since there is still a limiting voltage, more plans are being made to try to correct the situation.

The results that we have to date show that the system is capable of the resolution that we need in order to obtain a better value of the first energy levels of ^{57}Cu. Over the summer of 1993 we will be continuing the search.

Appendix A: Results of April Run

During the experimental run of April 9 to April 13, we were able to conduct several data collection sessions between problems with the velocity filter. The velocity filter developed the pattern of periodic shifts in the fields. With a steady current of 560.0 Amps registering through the magnetic coils, the electric potential had to be adjusted at times to place the signal on the silicon detector. The appropriate setting varied in discrete steps between 155 kV and approximately 130 kV. More work is being planned to correct this situation and any other problems that might have been covered up by it including internal sparking.

The data stored during the favorable periods were divided into two types: singles and coincidence. In a singles run, the only requirement for the computer to accept the signal from the detectors is that there be a signal from the silicon detector. In a coincidence run the computer would only accept the data if a signal came from the silicon and one of the three germanium detectors that were set up around the target chamber. This helps cut down the background of the spectra, but also involves longer run times for a similar amount of data as compared to a singles run. The longer times allows for the greater chance that the E-field in the velocity filter would need to be changed in order to avoid "washing-out" the

data as the particles scrolled across the detectors. Thus, despite the fact that 39 data runs were actually recorded, there were only four coincidence runs that were useful.

The four acceptable runs were summed together using the Q replay system. The position vs. energy spectrum is shown in Figure A1 for the sum of the runs.

Figure A1: POS vs. E for sum of four runs.

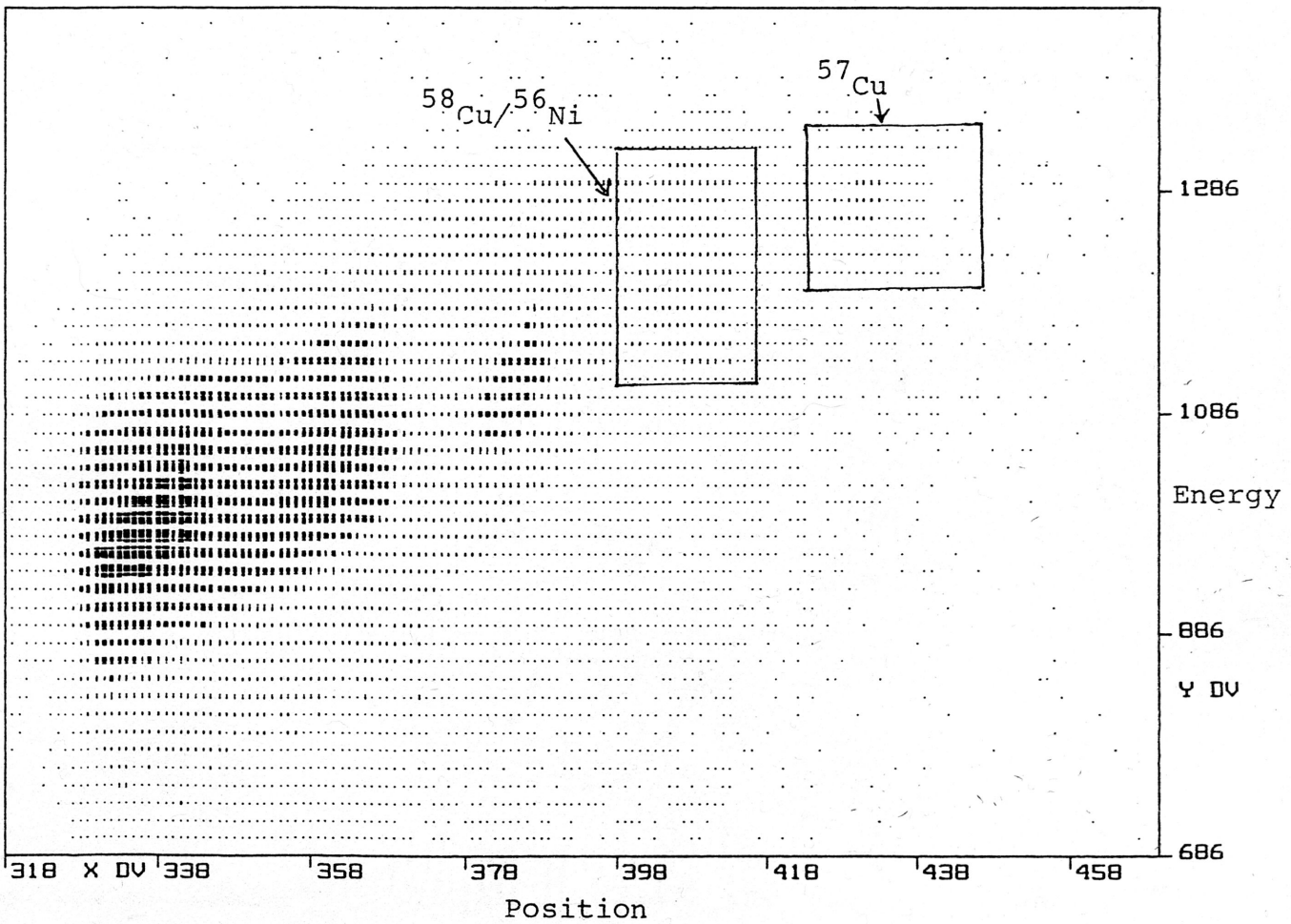

A gate was set on the $^{56}Ni/^{58}Cu$ group and the ^{57}Cu group, as indicated in the diagram, in order to replay the runs and select only those events that we are reasonably confident were

one of these particles. The low count rate for the sum of the four runs (only 193,000 events total) does not provide sufficient statistics for us to see any peaks corresponding to γ-lines in the germanium spectra. With the modifications that are being carried out on the velocity filter, longer data collection sessions will be possible when we are able to run again. Another run has been tentatively scheduled for late May.

Bibliography

[1]C. A. Gagliardi, D. R. Semon, R. E. Tribble, and L. A. Van Ausdeln, Phys. Rev. C 34, 1663 (1986).

[2]B. Sherrill *et al.*, Phys. Rev. C 31,875 (1985).

[3]T. Shinozuka *et al.*, Phys. Rev. C 30,2111 (1984).

[4]B. G. Harvey. *Introduction to Nuclear Physics and Chemistry*, Prentice-Hall, Inc.: Englewood Cliffs, NJ, 1969. p. 123.

[5]R. Eisberg and R. Resnick. *Quantum Physics of Atoms, Molecules, Solids, Nuclei, and Particles*, John Wiley & Sons: New York, 1985. p. 579.

[6]Ibid, p. 580.

[7]F. Shu. *The Physical Universe*, University Science Books: Mill Valley, CA, 1982. p. 116.

[8]H. Bethe. *Highlights of Modern Astrophysics*, edited by S. L. Shapiro and S. A. Teukolsky, John Wiley & Sons: New York, 1986. p. 56.

[9]F. Shu. p. 120.

[10]R. K. Wallace and S. E. Woosley, Astrophys. J. Suppl. 45, 389 (1981).

[11]D. H. Youngblood, et. al. *Momentum Achromat Recoil Spectrometer: A Proposal to Supplement Grant DE-FG-05-86ER40256*, Submission to Office of High Energy and Nuclear Physics, 1988. p. 9.

[12]Ibid, p. 53.